Available online at www.sciencedirect.com
SCIENCE DIRECT
Polymer 47 (2006) 1150–1158
polymer
www.elsevier.com/locate/polymer

Surface properties of poly(dimethylsiloxane)-based inorganic/organic hybrid materials

Zhili Li [a], Wei Han [b], Dimitry Kozodaev [c,d], José C.M. Brokken-Zijp [a,*], Gijsbertus de With [a], Peter C. Thüne [b]

[a] *Laboratory for Materials and Interface Chemistry, Eindhoven University of Technology, P.O. Box 513, 5600 MB Eindhoven, The Netherlands*
[b] *Laboratory for Physical Chemistry of Surfaces, Eindhoven University of Technology, P.O. Box 513, 5600 MB Eindhoven, The Netherlands*
[c] *Laboratory for Macromolecular Chemistry and Nanoscience, Eindhoven University of Technology, P.O. Box 513, 5600 MB Eindhoven, The Netherlands*
[d] *NanoTechnology Instruments Europe BV, Apeldoorn, The Netherlands*

Received 1 November 2005; received in revised form 16 December 2005; accepted 16 December 2005
Available online 10 January 2006

Abstract

Poly(dimethylsiloxane) (PDMS)-based hybrid materials were prepared by the sol–gel method on Si wafers, Al and polystyrene (PS) substrates. The reaction was monitored by attenuated total reflectance-infrared (ATR-IR) spectroscopy. The hybrid materials have always one surface made in contact with air and one with a substrate. These surfaces were investigated by using tapping mode atomic force microscopy (AFM), X-ray photo-electron spectroscopy (XPS), low-energy ion scattering (LEIS) and dynamic contact angle (DCA) analysis. The hybrid sample surfaces made in contact with air and substrates appeared to have different structures. The former have a silica-free PDMS top layer of ~2 nm thick; while in the latter cases, SiO_2 are located at or just beneath the outermost atomic layer. In air and at room temperature, SiO_2 are likely beneath the outermost atomic layer. In contact with water, polar –OH groups at the surface of SiO_2 can easily stretch out to the outermost atomic layer. No correlation was found between the roughness of the surfaces and the amount of in situ formed SiO_2 present in the materials.

Keywords: Poly(dimethylsiloxane); Inorganic/organic hybrids; Surface property

1. Introduction

Inorganic/organic hybrid materials prepared by the sol–gel method have received more and more attention in the past 20 years. The combination of organic and inorganic components gives these materials versatility in composition, structure and properties, which makes them very competitive and promising materials for applications in many fields such as optics, electronics, mechanics, sensors, and catalysis [1,2].

As an important family of the hybrid materials, poly(-dimethylsiloxane) (PDMS)-based hybrids are widely used as insulating materials, in medical devices, as membrane, in optical parts and antifouling and water-repellent coatings. Since early 1980s, Mark et al. [3–5] first 'borrowed' the sol–gel method from the inorganic chemistry to prepare PDMS networks containing in situ precipitated silica, this kind of inorganic/organic hybrid materials has been intensively studied on their preparation [6–10], their mechanical properties [7–12], thermal stability [7,10,11], hydrophobicity [13,14] and transparency [15–17].

Currently, these PDMS-based materials are used as model hybrid networks for our study on the adhesion of polymer coatings. Evidently, the surface and near surface composition, structures and morphologies are the dominating factors controlling their surface properties and adhesion behavior. However, in the literature, this field was seldom addressed and only very few studies [13,18,19] investigated these properties. Shindou et al. [13] studied the effects of heat-treatment temperature on the surface properties and surface morphologies of PDMS-based hybrid materials by using contact angle measurements and atomic force microscopy (AFM). They reported that the surface homogeneity changed before and after the heat-treatment at 300 °C. Martos et al. [18] used inverse gas chromatography to measure the surface energy of silica–TEOS–PDMS hybrids with 60 wt% inorganic component. They reported that the amount of PDMS was not enough to cover all silica surfaces, resulting in different surface energies of the surfaces originating from the presence of

* Corresponding author. Tel.: +31 40 2473742; fax: +31 40 2445619.
E-mail address: j.brokken@tue.nl (J.C.M. Brokken-Zijp).

0032-3861/$ - see front matter © 2005 Elsevier Ltd. All rights reserved.
doi:10.1016/j.polymer.2005.12.057

hydroxyl groups on silica surfaces. In contrast, Han et al. [19] added a small amount of PDMS to their system. They claimed that during the sol–gel process, the hydrophobic PDMS tended to be localized at the surface, thereby lowering the free energy of the system. These statements are incomprehensive and even contradictory at some points, making it very difficult to understand how the surface properties, such as adhesion, are controlled by the chemical and physical factors such as surface composition, structures and morphologies of these hybrids. To do so, it is necessary to have deeper and broader understanding of the surface science of these materials.

This present paper focuses on the study on the surfaces of PDMS-based inorganic/organic hybrid materials prepared by the sol–gel method. We investigated the bulk and surface composition, structure and morphology of the hybrids with different amounts of inorganic components. Furthermore, we also studied the surface structures for hybrid surfaces made in contact with air and substrates, respectively.

2. Experimental

2.1. Materials

Tetraethyl orthosilicate (TEOS), silanol-terminated poly (dimethylsiloxane) (PDMS) with a number-average molecular weight of 4200, vinyl-terminated PDMS with a number-average molecular weight of 6000 (MWD = 2.07), and tetrakis(dimethylsiloxy)silane were purchased from ABCR, Germany. *cis*-Dichlorobis(diethyl sulfide)platinum(II) was obtained from Strem Chemicals. All materials were used without further purification.

2.2. Sample preparation

The hybrid samples were prepared via the sol–gel method. Silanol-terminated PDMS was mixed with TEOS with different molar feed ratios $r = [OEt]/[OH]$, where the OC_2H_5 groups are on the TEOS and the OH groups are chain ends on the PDMS (each TEOS molecule has four –OEt groups and each PDMS molecule has two –OH groups). After the solution was stirred for 10 min, two catalysts, dibutyltin diacetate and stannous 2-ethyl hexanoate, were added into the solution with concentrations of 1.0 and 1.7 wt% of the PDMS, respectively. The mixture was stirred for another 10 min, degassed and cast into a polystyrene (PS) petri-dish to gel at room temperature in air for 48 h and then at 50 °C under vacuum for another 24 h. Some samples were also cast onto silicon wafers and Al substrates using the same preparation method. The sample surfaces exposed to air were named as A-*, and sample surfaces contacting PS, Al and Si wafer as PS-*, Al-* and Si-*, respectively. For example, A-r30 represents a sample prepared with the molar feed ratio r of 30 and the surface studied is the one exposed to air. No water was added to the reaction mixtures except as was absorbed by the samples from the humidity in the air [4,17]. All samples were ca. 1 mm thick, transparent, rubbery and can be easily peeled off from the substrates.

A reference sample exposed to air, denoted as Ref-PDMS, was prepared by cross-linking vinyl-terminated PDMS and tetrakis(dimethylsiloxy)silane with *cis*-dichlorobis(diethyl sulfide)platinum(II) as the catalyst, as shown in Scheme 1. The mixture was cast into a polystyrene petri-dish to cure at 60 °C for 3 days under vacuum. This sample is used as reference sample (0% SiO_2), because it is cross-linked through hydrosilylation reaction, thus a pure soft PDMS network is formed.

2.3. Methods

The densities of the samples were determined by pycnometry. The weight concentrations of SiO_2 are calculated from density data using values of $d = 0.96\ g/cm^3$ for PDMS networks and $d = 2.2\ g/cm^3$ for silica [20]. The effective moduli (E_{eff}) near the surface ($\sim 10\ \mu m$) of the samples were measured in air at room temperature using micro-indentation with a Berkovich indenter following a procedure described elsewhere [21,22].

Attenuated total reflectance-infrared (ATR-IR) spectroscopy was performed using a BIORAD Excalibur Spectrometer at room temperature. All spectra were recorded under dry N_2 at room temperature between 4000 and 650 cm^{-1} with a resolution of 2 cm^{-1} co-adding 30 scans. All spectra were

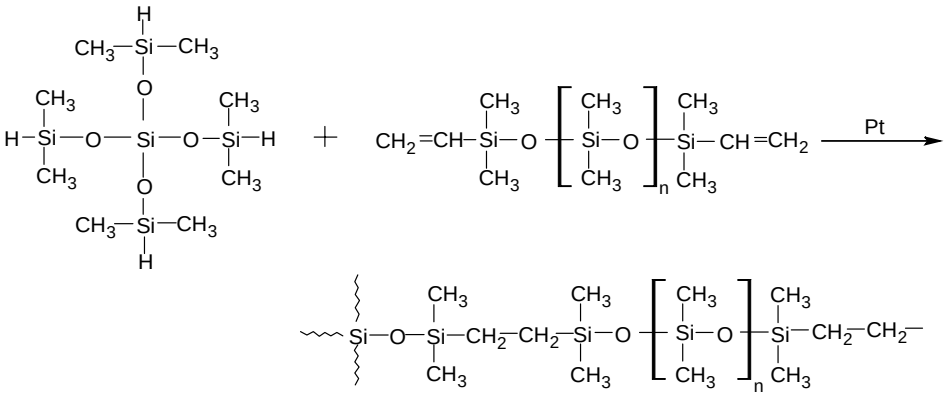

Scheme 1.

normalized by the C–H bending band of the PDMS backbone located at 1259 cm^{-1}.

The cross-sectional morphologies of the samples were investigated using a Philips environmental scanning electron microscope XL-30 ESEM REG (Philips, The Netherlands, now FEI Co.). Imaging of the samples cross sections was performed in high-vacuum mode using acceleration voltages of 1 kV (low-voltage SEM, LVSEM) and a secondary electron (SE) detector.

Nanoscale morphological surface properties were measured by using AFM NTEGRA (NT-MDT, Moscow, Russia). The topography and phase images were obtained in the intermittent contact mode with Si-cantilevers, spring constant $k=5.5$ N/m (NSG01, NT-MDT, Moscow, Russia). A sample area of 1×1 μm^2 was scanned. The measurements were performed in air at room temperature at a humidity of 45–50%.

X-ray photo-electron spectroscopy (XPS) was conducted with a VG Escalab 200 using a standard aluminum anode (Al Kα 1486.3 eV) operating at 510 W. Spectra were recorded at room temperature at normal emission at background pressure of 5×10^{-10} mbar, at take-off angles of 15, 30 and 90° with respect to the plane of the sample. All binding energies were referenced to the C_{1s} peak at 284.6 eV [23].

Low-energy ion scattering (LEIS) experiments were performed under vacuum at room temperature with the Calipso instrument operated with a 3 keV $^3He^+$ ion beam that is most sensitive for low atomic number elements. The measurements were performed on specimen areas of 2×2 mm^2. The total ion dose used was of the order of 5×10^{13} ions/cm^2.

Dynamic contact angles (DCA) analysis was performed in air at room temperature using the sessile drop method [24] with an apparatus OCA30 (Dataphysics Instruments). Distilled water was used as the probe liquid. All advancing and receding contact angles given are the average value of at least five measurements on different positions of the sample.

3. Results and discussion

3.1. Material preparation

The synthesis of our hybrid materials by the sol–gel method involves the basic steps as shown in Scheme 2: hydrolysis of TEOS, the self-condensation of the –OH groups of hydrolyzed TEOS, the self-condensation of the –OH groups of silanol-terminated PDMS, and the co-condensation between the –OH groups of hydrolyzed TEOS and the –OH groups of silanol-terminated PDMS. As the self-condensation is going on, SiO_2 is precipitated in situ and thus a hybrid material is formed. The co-condensation between the –OH groups of PDMS and hydrolyzed TEOS results in chemical bonds between the SiO_2 and PDMS phase [4,25].

The sol–gel process was studied by ATR-IR spectroscopy. The disappearance of the –OEt group of TEOS was followed by measuring the change in the Si–OEt stretching bands (1167, 1072 and 957 cm^{-1}) [26] and the C–H stretching bands of the ethyl groups (2976, 2930 and 2890 cm^{-1}). The C–H bending bands of ethyl groups of TEOS are located in the range of 1350–1480 cm^{-1}. The spectra of r30 sample after varying curing time are presented in Fig. 1(a). All these bands decrease during cure as expected and are no longer visible after cure, showing that the hydrolysis of –OEt groups of TEOS is (almost) complete after cure.

Fig. 1(b) shows the ATR-IR spectra of the samples made using different r values after cure for 3 days. It is known from literature that precipitated SiO_2 has a strong band at 1080 cm^{-1} and a very broad shoulder at about 1220 cm^{-1} [26]. As shown in this figure, an increase in these two bands indicates that when higher amounts of TEOS are present in the formulation, more SiO_2 is precipitated, in line with literature [4,6]. A weak broad absorption band at around 3400 cm^{-1} assigned to OH stretching was observed. This band can originate from water

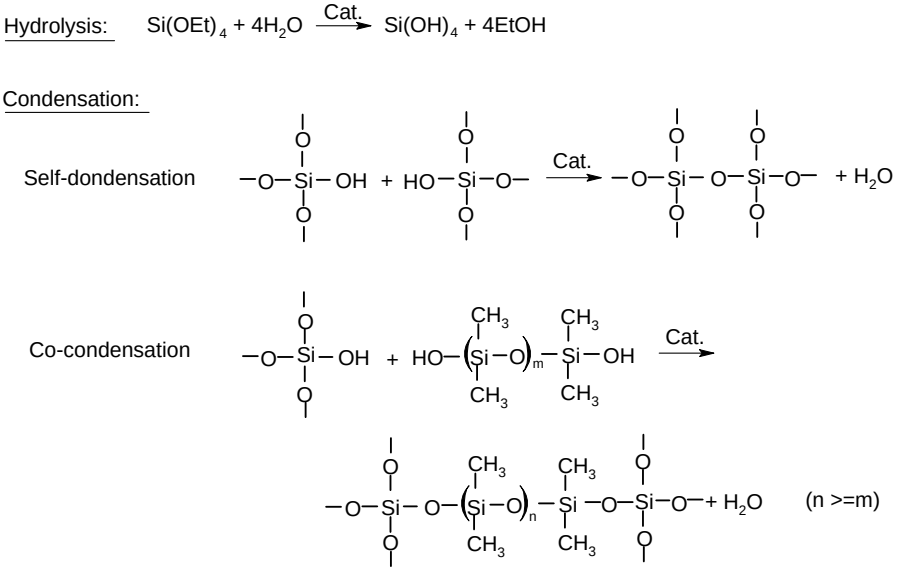

Scheme 2.

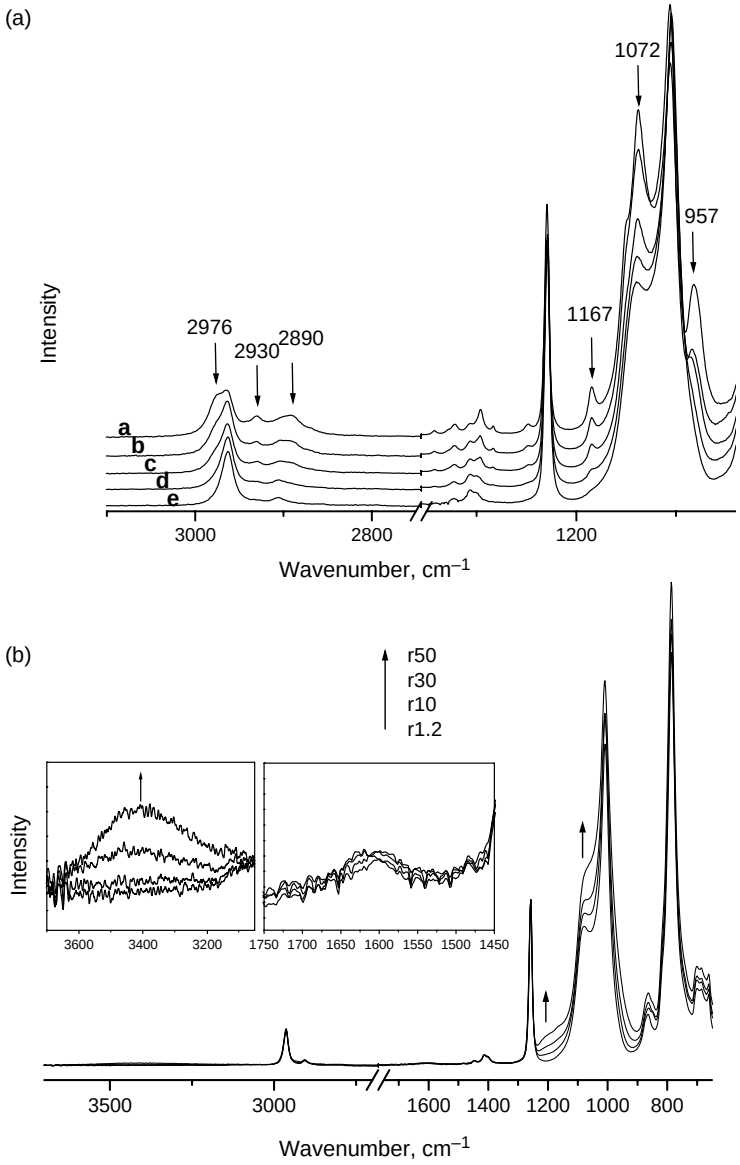

Fig. 1. (a) ATR-IR spectra of the r30 sample with increasing curing time (a) 0 min; (b) 18 min; (c) 38 min; (d) 68 min and (e) 148 min. (b) ATR-IR spectra of the cured samples (cure for 3 days) with different molar feed ratio r (r=1.2, 10, 30, 50). The arrow direction shows the increase in r.

molecules or hydro-bonded Si–OH groups [27]. A very weak band centered at 1630 cm^{-1} assigned to bending of the water molecules showed the presence of a trace of water [28]. However, this band is fairly constant for all samples, indicating that the increase in the band at around 3400 cm^{-1} with increasing r values originates from the increase of Si–OH groups. This agrees with literature that polar –OH groups are present at the surfaces of SiO_2 [29–31].

The cross-sectional morphologies of the samples were investigated by LVSEM. An example of r30 sample was shown in Fig. 2. The homogeneously dispersed SiO_2 particles have a size of about 50–200 nm. There are some small SiO_2 aggregates (<1 μm) present in the samples.

The increase in the amount of precipitated SiO_2 with increasing molar feed ratio r was confirmed by density measurements on the cured samples (Table 1). The larger the r, the larger the density is. Using the difference in density between

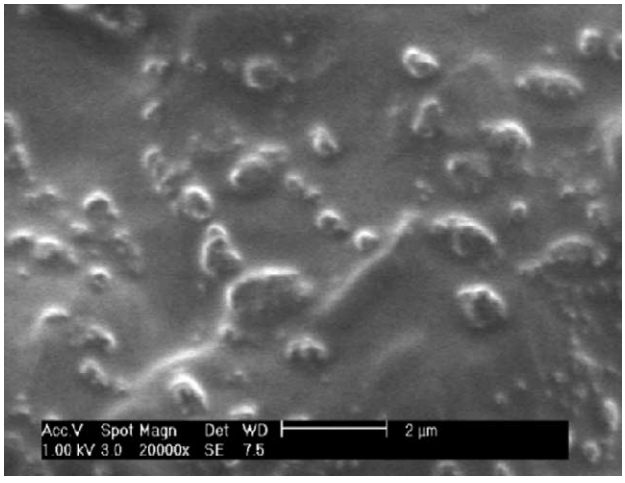

Fig. 2. LVSEM image of the cross section of r30.

Table 1
Bulk properties of the hybrids

r^a	Density (g/cm^3)	SiO_2 (wt%)	E_{eff} (MPa)
Ref-PDMS	0.959	0	1.2
1.2	0.969	0.80	1.3
2.5	0.986	2.18	2.5
6	1.001	3.39	5.2
10	1.014	4.44	5.9
20	1.040	6.54	8.0
30	1.066	8.64	12.8
50	1.137	14.3	27.6

[a] Molar feed ratio r=[OEt]/[OH].

PDMS phase and precipitated SiO_2 phase, the bulk weight concentrations of SiO_2 of all samples were determined. A gradual increase in concentration with increasing r was observed, which is in agreement with our ATR-IR results reported above. The effective elastic moduli of samples, listed in Table 1, increase with r, in line with our knowledge of the reinforcement effects of inorganic fillers on a rubbery material [4,6,25].

3.2. Surface properties of the hybrid materials

The adhesion between two materials is influenced strongly by the chemical composition and morphology at the surfaces of the materials. In order to study the morphologies and chemical

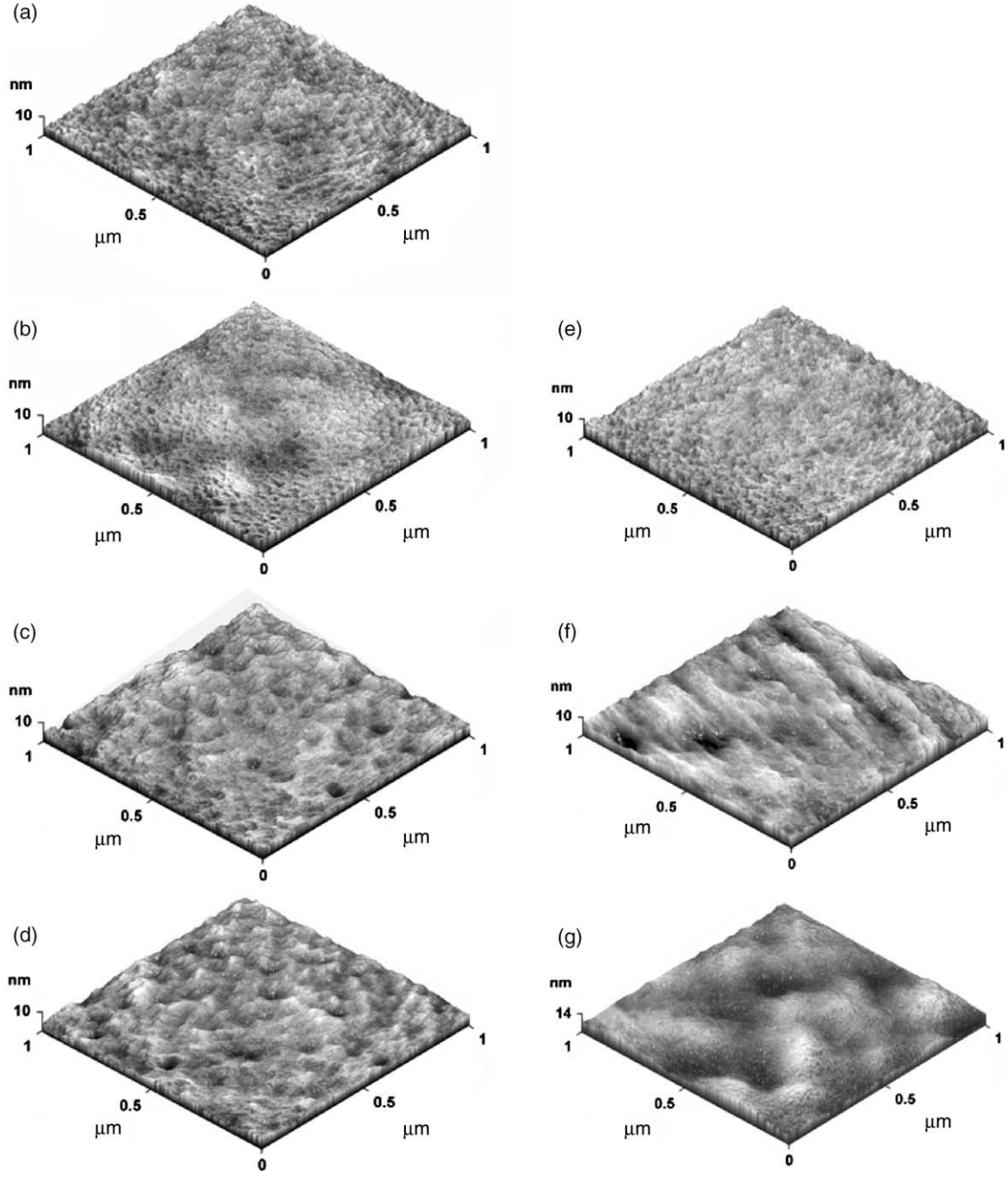

Fig. 3. AFM topography mapping images of (a) A-r1.2; (b) A-r10; (c) A-r30; (d) A-r50; (e) Si-r50; (f) Al-r50 and (g) PS-r50.

Table 2
Data of AFM and LEIS measurements

Sample	AFM, R_a[a] (nm)	LEIS, peak area (%)		
		C	O	Si
Ref-PDMS	3.6	25	17	58
A-r1.2	2.1	25	17	58
A-r50	3.1	25	17	58
Si-r50	2.6	27	15	58
Al-r50	7.8	27	16	57
PS-r50	10.5	27	15	58

[a] Averaged roughness.

composition of these surfaces in more detail, a combination of AFM, XPS, LEIS and DCA analyses were used to investigate the surface properties.

The morphologies at a nanometer level of the sample surfaces were studied by using AFM, as shown in Fig. 3. The averaged roughnesses of several surfaces were listed in Table 2. A- and Si- surfaces have similar averaged roughnesses of 2–4 nm, indicating a very smooth surface and no dependency of the roughness of the samples on the amount of SiO_2 present in the materials was found. Al- and PS-surfaces have a higher roughness. This difference originates from the roughness of the Al and PS substrates themselves, because the patterns shown are those of an Al and PS substrate.

Also the phase images of the different surfaces were given for materials made with different amounts of SiO_2. Fig. 4 shows the phase images of Ref-PDMS, A-r50 and Si-r50. Here again no correlation was found between the roughness of the samples and the amount of particles present. The observed variation in roughness may be explained by the increase in the amount of ethanol evaporated from the material during the preparation of the samples. Using the AFM nanoscale force–distance mode these materials will be studied in more depth later on.

XPS was used to determine the atomic composition of the outmost 10 nm of the sample surfaces. Measurements were performed at take off angles of 90, 30 and 15°, giving the estimated depths of penetration of about 10, 5 and 2 nm, respectively. For all samples, the binding energy for C_{1s}, O_{1s} and Si_{2p} were observed at 284.6, 532.1 and 102.1 eV, respectively. The silicon-to-oxygen configuration has a particular Si_{2p} binding energy that is dependent on the number of oxygen atoms bonded to a silicon atom. The Si_{2p} binding energy shifts to a higher value when more oxygen atoms are bonded to the silicon atom. The Si_{2p} peak at 102.1 eV is assigned to an organic silicone phase and the peak at 103.8 eV is assigned to Si atoms bonded to three or four oxygen (SiO_x, $x=3$, 4) [23,32]. For sample surfaces in contact with air (A-r1.2, A-r30 and A-r50), the amount of C decreases and O increases with an increase in molar feed ratio r, indicating that more SiO_2 is precipitated in the top layer of 10 nm when a higher r value is applied in the formulation (Table 3). This is confirmed by the increase of the Si_{2p} peak area at 103.8 eV in respect to the peak area at 102.1 eV with increasing r. It deserves to be noticed that for the A-r1.2 and Si-r1.2 samples, no peak for the silica-like phase is found, showing that in the ~10 nm top layer, no silica is present. When the penetration depth is ~5 nm, some silica was still found for the A-r30 and A-r50 samples, but the amount was less than the value calculated over a depth of 10 nm. No silica was found in these samples at the top layer of ~2 nm. These results clearly show that for the surfaces made in contact with air, only PDMS is present at the 2 nm top layer of these surfaces. The amount of SiO_2 increases gradually from this top layer, however, even at 10 nm depth, the amount of SiO_2 is less than that in the bulk of the samples.

For the sample surfaces made in contact with substrates, the atomic composition is different from the surfaces made in contact with air. As listed in Table 3, Si-r50, Al-r50 and PS-r50 samples contain less carbon and more oxygen atoms. Putting aside the difference between the calculated atomic ratio for PDMS (C:O:Si=50:25:25) and our measured value for Ref-PDMS (C:O:Si=49:31:20), the atomic compositions of these three samples, compared to A-r50, are more close to the bulk value (C:O:Si=37:36:27) calculated from

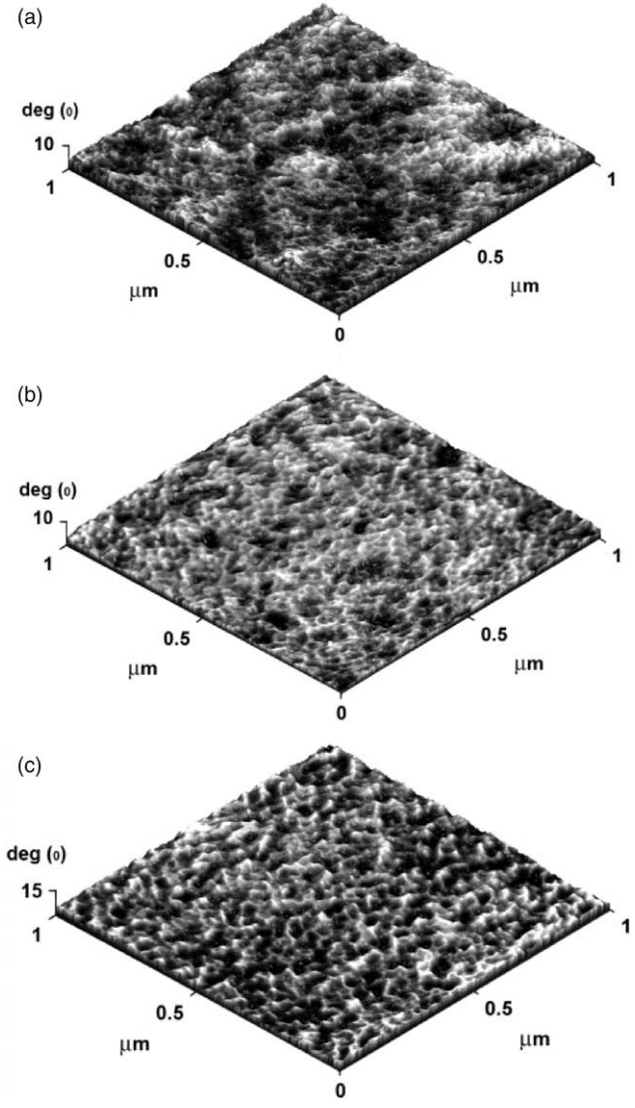

Fig. 4. AFM phase images of (a) Ref-PDMS; (b) A-r50 and (c) Si-r50.

Table 3
Results of XPS measurements

Sample	Take off angle (°)	Atomic composition (%)[a]			Peak area (%)	
		C	O	Si	Si_{2p} (SiO_z) (103.8 eV)	Si_{2p} (PDMS) (102.1 eV)
Ref-PDMS	90	49	31	20	0	100
	15				0	100
A-r1.2	90	49	32	19	0	100
	15				0	100
Si-r1.2	90	49	32	19	0	100
	15				0	100
A-r30	90	47	36	17	10	90
	30				2	98
	15				0	100
A-r50	90	45	37	19	15	85
	30				5	95
	15				0	100
Si-r50	90	39	40	20	25	75
	30				22	78
	15				20	80
Al-r50	90	41	39	20	20	80
	30				18	82
PS-r50	90	42	38	20	20	80
	30				18	82
	15				15	85

[a] Calculated from atomic sensitivity factors for X-ray sources [33].

weight fraction of SiO_2. A comparison of the Si_{2p} binding energy of sample A-r50 (a–c) and Si-r50 (d–f) is shown in Fig. 5. The Si_{2p} peak area at 103.8 eV assigned to the inorganic silica-like phase is still present in the Si-r50 sample even when a penetration depth of ~2 nm is applied. The variation found in Si_{2p} areas at 103.8 eV at different penetration depth is within the fault of measurement (~5%), suggesting that for the sample surfaces made in contact with substrates, the distribution of SiO_2 phase is homogeneous from bulk to the top surface (~2 nm).

DCA analysis and LEIS were performed to investigate the properties of the outermost surface layer. It is known that the contact angle depends on both the chemical composition of the surface and the surface roughness of the micrometer level [34]. The averaged roughness data (Table 2) show that all the tested surfaces are smooth with a roughness lower than ~10 nm, thus we assume that any change of contact angles results from the chemical composition change. The contact angles with water of samples made in contact with air and substrates, from different molar feed ratio *r*, are listed in Table 4. The advancing contact angles of surfaces in contact with air (A-r1.2, A-r10, A-r30 and A-r50) are kept constant at ~105°, very close to the values of 106.6° measured for Ref-PDMS. Hyteresis is also stable. This is in agreement with our previous XPS finding that these surfaces have a silica-free thin top layer of PDMS. For

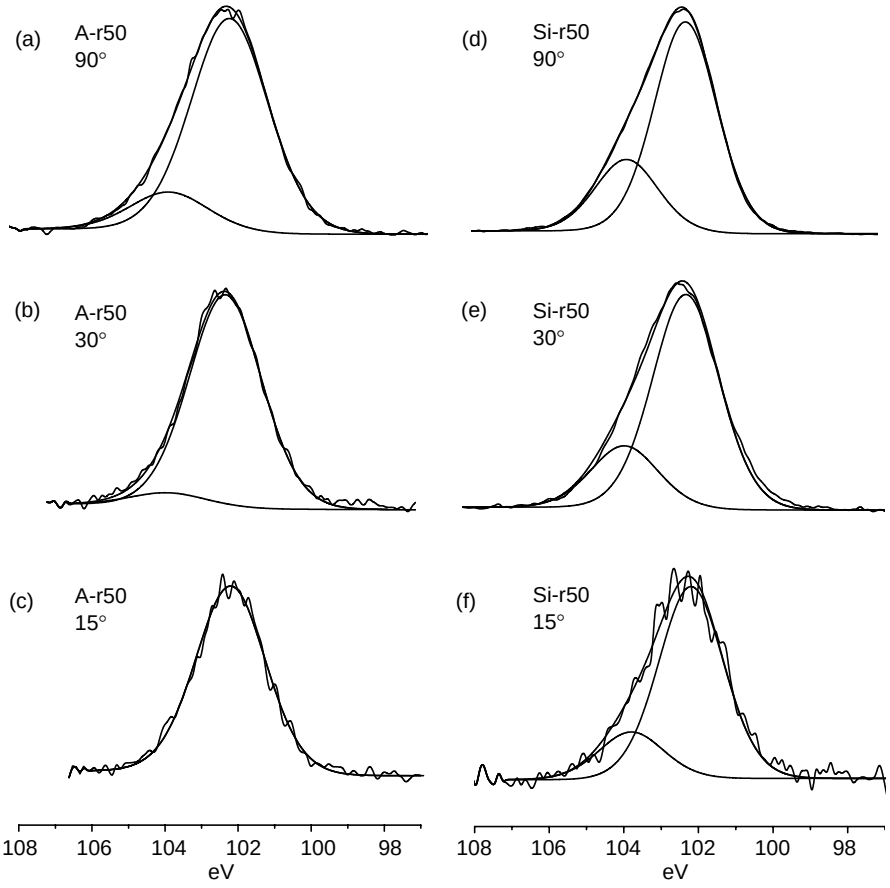

Fig. 5. XPS spectra of A-r50 at take off angles of (a) 90°; (b) 30° and (c) 15° and Si-r50 at (d) 90°; (e) 30° and (f) 15°. The Si_{2p} peak is resolved into the organic silicone 102.1 eV peak and the inorganic silica-like 103.8 eV peak.

the surfaces in contact with substrates, the advancing contact angles decrease with increasing r, to $\sim 92^\circ$ when r is 50. At the same time, hysteresis increases with the increasing in r. There are two possibilities that can cause this change of contact angles. Some hydrophilic SiO_2 exist at the surfaces and/or the SiO_2 phases are located just beneath the outermost atomic layer. It is unlikely that SiO_2 are located at the outermost layer because of its high surface energy and the flexibility of the PDMS chains, thus we may assume that the SiO_2 phases are beneath the outermost atomic layer. When the surface contacts with water, the –OH groups at the surface of SiO_2 may extend towards the interface of water and the hybrid sample, this will make the sample surface less hydrophobic. To prove the above assumptions, we did LEIS experiments to study the chemical composition of the outermost atomic layer. The peak areas percentage of C, O and Si of different samples (Table 2) show very small differences. This seems to prove the above assumptions. Unfortunately, we cannot exclude that the error of measurements of LEIS is too large for observing these differences. Moreover, LEIS measurements were done under vacuum without the presence of moisture that may have enhanced the formation of a silica-free outermost atomic layer during our LEIS experiments.

Based on above studies, we propose two different surface structures for hybrid surfaces made in contact with air and with substrates, respectively. For the surfaces made in contact with air, there is a ~ 2 nm thick silica-free layer of PDMS at the surface, giving a surface properties similar to the pure PDMS. For the surfaces made in contact with substrates, the precipitation of SiO_2 may happen directly at the interfaces. The reasons for this difference in the presence of SiO_2 at the surface might be complex. We believe that surface energies of PDMS, SiO_2, and substrates do play an important role, but other factors such as the difference in the amount of water present on the substrates may be important too. After the samples are peeled off from the substrates, it seems to be more likely that because of the flexibility of PDMS chains, migration of PDMS chain to the outermost atomic layer may occur, [35,36] by which polar –OH groups present at the surface of SiO_2 are covered with PDMS. When these surfaces meet water as what happened in the DCA experiments, these –OH groups can easily stretch out, resulting in lower contact angles. We expect the two different structures of these hybrid material surfaces will shed more light on our current adhesion studies on these materials.

Table 4
Dynamic contact angles of A-, Si-, Al- and PS- samples with different molar feed ratio r ($r = 1.2$, 10, 30, 50)

Samples	θ_{adv} (°)	θ_{rec} (°)	Hysteresis (°)
Ref-PDMS	106.6	101.9	4.7
A-r1.2	105.3	100.3	5.0
Si-r1.2	104.2	99.2	5.0
Al-r1.2	105.6	100.7	4.9
PS-r1.2	105.4	100.5	4.9
A-r10	105.4	100.6	4.8
Si-r10	95.3	89.5	5.8
Al-r10	97.8	92.7	5.1
PS-r10	97.9	92.9	5.0
A-r30	105.1	99.7	5.4
Si-r30	93.6	84.8	8.8
Al-r30	94.0	86.0	8.0
PS-r30	94.3	85.4	8.9
A-r50	104.7	99.4	5.3
Si-r50	91.3	81.4	9.9
Al-r50	92.4	81.7	10.7
PS-r50	92.9	83.1	9.8

4. Conclusions

PDMS-based inorganic/organic hybrid materials were prepared by the sol–gel method on Si wafer, Al and PS substrates. The reaction was followed by ATR-IR. The morphologies of hybrid surfaces made in contact with air and different substrates were characterized by AFM using the intermittent contact mode. All surfaces are homogenous and smooth. XPS, LEIS and DCA analysis were used to investigate the properties of the surfaces. The results obtained by these techniques match each other. The top surface structures of the hybrid surfaces made in contact with air and substrates are different. The former have a silica-free PDMS top layer of ~ 2 nm thick; while in the latter cases, SiO_2 are more likely located beneath the outermost atomic layer, and polar –OH groups at the surface of SiO_2 can easily stretch out to the outermost atomic layer when the surfaces contact with polar groups. No correlation was found between the roughness of the surface layers and the amount of SiO_2 particles present just beneath the outermost surface layer. Systemic study on the adhesion of such hybrid materials is on the way.

Acknowledgements

The authors would like to thank Dr W. Ming for his great help concerning DCA measurements and useful discussions. We appreciate Dr X. Zheng (TU/e, now Zhengzhou University, China) for performing the LVSEM measurements and Mr A. Knoester for performing the LEIS measurements and for helpful discussions. This research is partly funded by the Dutch Polymer Institute (Project 421).

References

[1] Sanchze C, Ribot R. New J Chem 1994;18:1007.
[2] Schmidt H, Seiferling B. Mater Mater Res Soc Symp Proc 1986;73:739.
[3] Mark JE, Pan S. J Makromol Chem Rapid Commun 1982;3:681.
[4] Mark JE, Jiang CY, Tang MY. Macromolecules 1984;17:2613.
[5] Mark JE, Ning YP. Polym Bull 1984;12:413.
[6] Huang H-H, Orler B, Wilkes GL. Macromolecules 1987;20:1322.
[7] Mackenzie JD, Huang Q, Iwamoto T. J Sol–Gel Sci Technol 1996;7:151.
[8] Guermeur C, Lambard J, Gerard J-F, Sanchez C. J Mater Chem 1999;9:769.
[9] Babonneau F, Maquet J. Polyhedron 2000;19:315.

[10] Iwamoto T, Morita K, Mackenzie JD. J Non-Cryst Solids 1993;159:65.
[11] Mackenzie JD. J Sol–Gel Sci Technol 1994;2:81.
[12] Kramer SJ, Mackenzie JD. Mat Res Soc Symp Proc 1994;346:709.
[13] Shindou T, Katayama S, Yamada N, Kamiya K. J Sol–Gel Sci Technol 2003;27:15.
[14] Noll W. Chemistry and technology of silicones. London: Academic Press; 1960.
[15] Dire S, Babonneau F, Sanchez C, Livage J. J Mater Chem 1992;2:239.
[16] Franville AC, Mahiou R, Zambon D, Cousseins JC. Solid State Sci 2001; 3:211.
[17] Rajan GS, Sur GS, Mark JE, Schaefer DW, Beaucage G. J Polym Sci, Part B: Polym Phys 2003;41:1897.
[18] Martos C, Fubio F, Rubio J, Oteo JL. J Sol–Gel Sci Technol 2001;20:197.
[19] Han JT, Lee DH, Ryu CY, Cho K. J Am Chem Soc 2004;126:4796.
[20] Gidley DW, Marko KA, Rich A. Phys Rev Lett 1975;36:395.
[21] Soloukhin VA, Posthmus W, Brokken-Zijp JCM, Loos J, de With G. Polymer 2002;43:6169.
[22] Li Z, Brokken-Zijp JCM, De With G. Polymer 2004;45:5403.
[23] Hillborg H, Gedde UW. Polymer 1998;39:1991.
[24] Garbassi F, Morra M, Occhiello E. Polymer surfaces. New York: Wiley; 1994.
[25] Mark JE. Chem Tech 1989;19:230.
[26] Anderson DR. In: Lee Smith A, editor. Analysis of silicones. New York: Wiley-Interscience; 1974.
[27] Lee Smith A. Spectrochim Acta 1960;16:87.
[28] Julian B, Gervais C, Cordoncillo E, Escribano P, Babonneau F, Sanchez C. Chem Mater 2003;15:3026.
[29] Liu CC, Maciel GE. J Am Chem Soc 1996;118:5103.
[30] Gay ID, Mcfarlan AJ, Morrow BA. J Phys Chem 1991;95:1360.
[31] Tuel A, Hommel H, Legrand AP, Kovats SZ. Langmuir 1990;6:770.
[32] Toth A, Bertoti L, Blazso M, Manhegyi G, Bognar A, Azaplonczay X. J Appl Polym Sci 1994;52:1293.
[33] Wagner CD. Surf Interface Anal 1981;3:211.
[34] Eick JD, Good RJ, Heumann AW. J Colloid Interface Sci 1975;53:235.
[35] Everaert EP, Van Der Mei H, Busscher HJ. J Adhes Sci Technol 1996; 10:351.
[36] Kim SH, Cherney EA, Hackam R. IEEE Trans Power Delivery 1991;6:1549.